Dynamics of the Film produced by Spray Impact under Various Gravity Levels

O. Kyriopoulos*, I. V. Roisman and C. Tropea
Chair of Fluid Mechanics and Aerodynamics
Technische Universität Darmstadt
64287 Darmstadt, Germany

Abstract

The present experimental study is devoted to the investigation of spray impact onto a rigid wall under various gravity levels. A large diversity of phenomena is associated with the flow in the liquid film layer initiated by single drop impacts onto a target and their interactions, which is an element of spray impact. Due to the complexity of the problem, the hydrodynamics of the films created by sprays is not entirely understood and no reliable model describing exclusively the behavior of the liquid film or depicting spray cooling is present until now.

The main aim of the present study is to better understand the hydrodynamics under terrestrial, reduced gravity and hypergravity conditions. By focusing on the dynamics of the thin liquid film produced by spray impact in the wall region it is expected to provide a sound basis for a reliable modeling of spray cooling.

This phenomenon has been investigated under terrestrial conditions and compared with observations gained under zero gravity and hypergravity conditions. The experiments at zero gravity conditions have been performed during Parabolic Flight Campaigns and on board of the ballistic rocket TEXUS 45 with microgravity duration of 360 s. The hypergravity and reduced gravity experiments have been performed in a centrifuge.

Spray propagation and wall impact at various gravity levels have been observed using a high-speed video system. Spray parameters have been determined with the help of image processing. Moreover, image analysis and the statistical methods of analysis have been applied to estimate the typical thickness of the liquid layer created by spray impact.

It has been shown that the thickness of the thin liquid film decreases when the gravity component normal to the wall increases. The spray cooling efficiency generally increases when the liquid film is thinner.

Introduction

Spray impact occurs in many industrial applications involving multiphase flow of liquid drops in gas, such as internal combustion engines, gas turbines, in agricultural and medical applications, spray drying, spray coating and spray cooling. In certain cases, spray impact onto a rigid wall is desired, e.g. spray cooling [1, 2, 3], spray painting, spray coating, deposition of agricultural sprays whereas in other cases spray impact is undesirable but unavoidable, e.g. in internal combustion engines or in the devices for spray drying. Even though the processes involved in spray impact are very complex, Roisman et al. [4, 5] have distinguished and classified some frequently observable splash scenarios. Due to the complexity of the phenomena the modeling of spray impact mainly relies on empirical or semi-empirical correlations. A comprehensive review of such models can be found in Cossali et al. [6]. Although simplified models of spray impact have been applied in this work, such modeling is usually applicable only for a restricted range of parameters as used in the corresponding experiments [7]. Hence, a generalization of such models may not be considered as a universal prediction tool [5].

Further progress in this field of research can be only achieved when the hydrodynamics of spray impact can be better clarified and captured in the models. A robust method of characterization of the fluctuating film and its average film thickness profile has been already investigated in [8]. In the present study this method has been applied for various levels of gravity and for diverse spray parameters. In addition, this study focuses on the investigation of the different splash scenarios expecting that by investigating the influence of gravity on spray impact, the understanding of the studied phenomena can be improved.

Experimental Method

The *experimental setup* consists of the test cell (shown schematically in Figure 1) surrounded by several major subsystems: a liquid supply system provides the water to generate the spray, a gas supply system allows to ventilate

* Olympia Kyriopoulos, o.kyriopoulos@sla.tu-darmstadt.de

the chamber by a gas co-flow, the deposited liquid and gas are exhausted from the cell using the extraction system, an optical visualization system and an electronic measurement and control system that allows to vary the mass flow rate by changing the injection pressure in the water supply line. The experimental cell for the experiments has been designed and constructed by EADS Astrium.

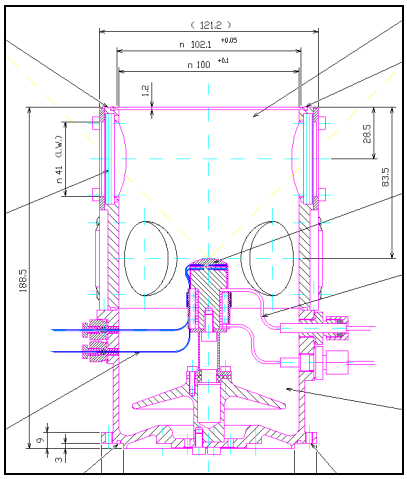

Figure 1. Mechanical drawing of the test cell including the target in the center.

The distilled water spray is generated by a full-cone pressure swirl atomizer (Spraying Systems 30° series) installed in the test cell at the distance of 70 mm from the convex heated target. The shape of the target is a truncated sphere of the diameter 20 mm. The nozzle and the target are installed in an experimental cell. The windows of the experimental cell are coated in order to attain a superhydrophobicity effect, which improves optical access [9].

The experiments at zero gravity conditions have been performed during Parabolic Flight Campaigns and on board of the ballistic rocket TEXUS 45 with microgravity duration of 360 s. The hypergravity and reduced gravity experiments have been performed in a centrifuge at ZARM (Center of Applied Space Technology and Microgravity, Bremen, Germany). For the centrifuge experiments the test cell has been positioned in different geometric configurations (see Figure 2) allowing us to investigate spray impact in the range of -20g to 20g.

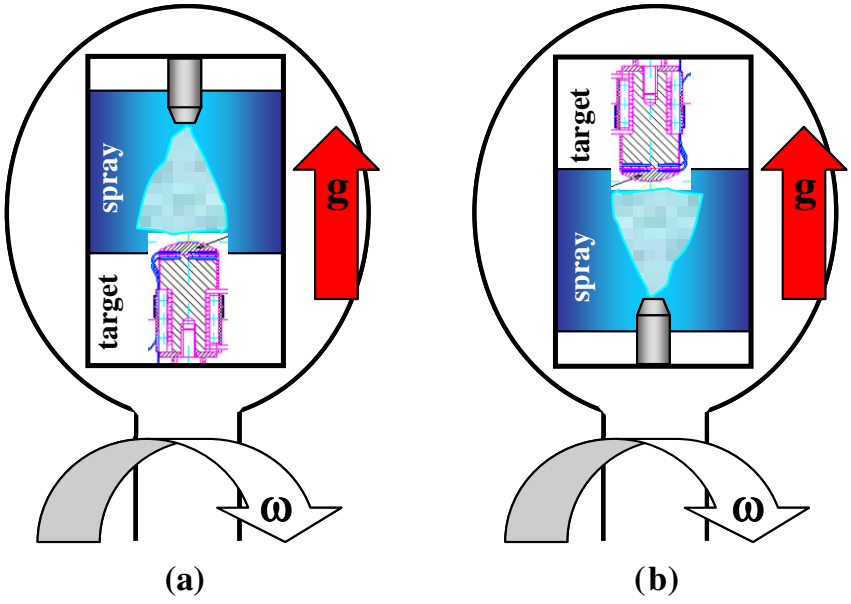

Figure 2. Experimental configurations for **(a)** negative and **(b)** positive ú-gravity condition.

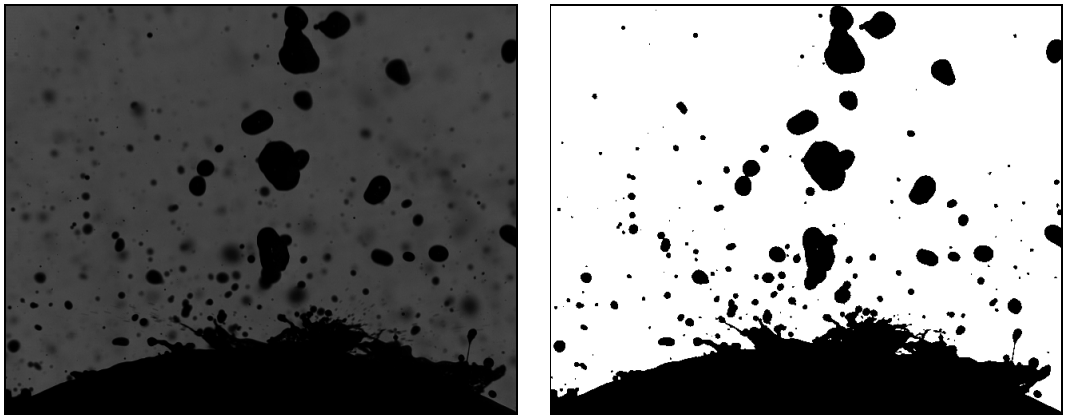

(a) **(b)**

Figure 3. (a) Captured image of spray impact and (b) processed black/white image at 2g and 0.25 l/min

During the centrifuge experiments the images of the spray/wall interaction have been captured with a frame rate of 16,000 fps using a high-speed video system consisting of a light source and a CMOS camera (Photron FASTCAM SA1). The high frame rates have allowed observation of several stages of the same splash event. The convex shape of the target provides the possibility to observe the contour of the free film surface at the target's generatrix.

Figure 3 a) shows the resulting image at a very high shutter speed (1/80,000 s) allowing clear identification of the spray impact. In order to analyze automatically the liquid film dynamics, the captured images have first been processed by enhancing the contrast (Fig. 3b.

From these b/w images important characteristics relevant to splash and film dynamics can be observed. The general aim is to identify characterizing parameters such as the total liquid film contour length, the film thickness distribution, or for characterization of crowns and jets (e.g. height and diameter evolution in time).

Results and Discussion

The first parameter to be discussed is the film thickness. In order to characterize the film thickness distribution the image processing procedure detects the contour of the wall film including the crowns and jets. The distance from a point of the liquid film contour to the corresponding nearest point at the surface of the dry target (contour-to-target-distance) is then calculated [8]. The average minimum contour-to-target-distance has been investigated under terrestrial conditions as well as during microgravity on board of a ballistic rocket and in addition during 2g phase of parabolic flight campaigns. By comparing the film thickness results from [9] with the ones at various gravity levels we obtain the tendency that the thickness of the thin liquid film decreases when the gravity component normal to the wall increases. Since the spray cooling efficiency increases when the liquid film is thinner [10], spray cooling should be more efficient at hypergravity. The decrease of the film thickness corresponds to a higher liquid velocity and thinner temperature boundary layer and, therefore, higher heat transfer coefficients.

In the second part of this study the spray propagation and wall impact observed by using a high-speed video system at various gravity levels are analyzed. Figure 4 shows a spray impacting onto the convex target at a constant flow rate of 0.25 l/min but for different gravity levels: from the maximal hypergravity condition +20g and +2g to 2g and the minimum gravity condition -20g. What we can see in this figure is that the spray behaves completely different although the water flow rate is constant.

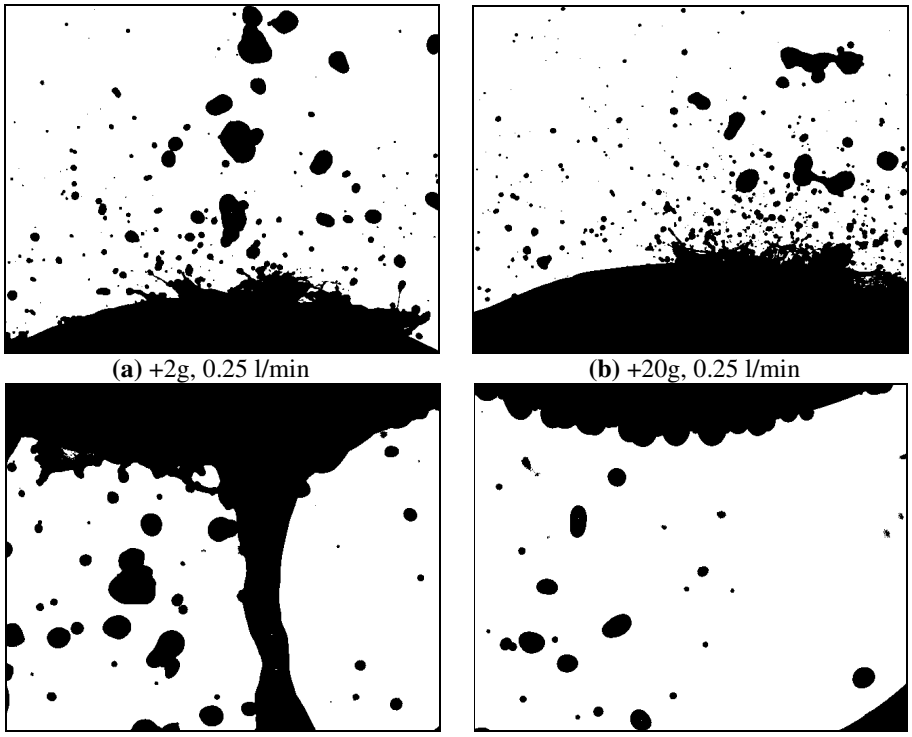

(a) +2g, 0.25 l/min **(b)** +20g, 0.25 l/min

(c) -2g, 0.25 l/min **(d)** -20g, 0.25 l/min

Figure 4. Spray impact dynamics at various gravity levels.

In Figure 4 (a) and (b) the spray appears comparable but the qualitative evaluation of the impacting drops shows that the average impact velocity U_a increases significantly at higher gravity levels. This trend is common throughout the entire range of water flow rate (see Figure 5). At the highest flow rate this dependence is less and the drop velocity is determined to a large extent by the velocity of the droplet at the nozzle exit.

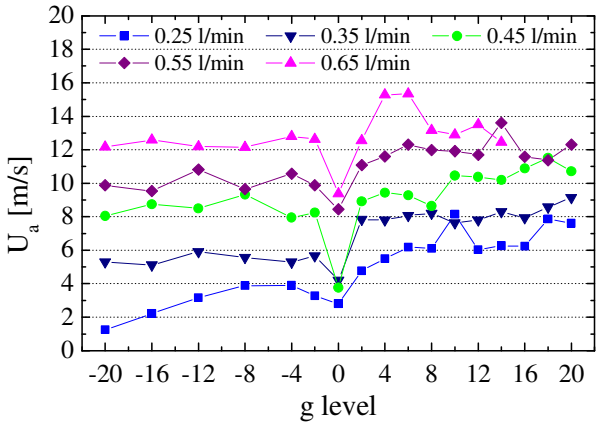

Figure 5. Average drop velocity at various gravity levels.

Unlike Figure 4 (a) and (b), the generated liquid film in Figure 4 (c) jets down like a filament whereas in (d) basically no drop reaches the target. At moderate negative hypergravity conditions the drops experience centrifugal forces away from the target and the secondary spray after impacting forms a jet-like structure. This will be denoted

film jetting. Compared to Figure 4 (d) and referring to the same gravity level of -20g, film jetting can be also observed at higher flow rates in Figure 6 (a) and (b).

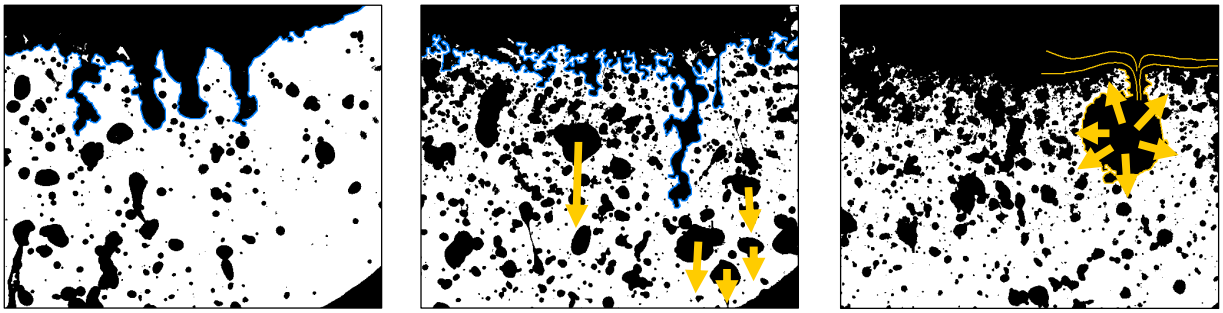

(a) -20g, 0.35 l/min **(b)** -20g, 0.55 l/min **(c)** -2g, 0.55 l/min

Figure 6. Secondary spray effects at various spray impact parameters.

The captured images show that at higher flow rates there are more finger-like filaments appearing from the liquid film. It also looks as if that there are more but thinner and smaller film jets developing with an increase of the water flow rate. Another effect that can be observed is the break-up of the film jetting at higher flow rates leading to larger secondary drops. Figures 6 (b) and (c) for instance, suggest that at -20g the secondary drops pinch off sooner from the film jets. There are more drop formations than at -2g but in addition those drops are much smaller. Taking a closer look at Figure 6 (c), at -2g the body force is not sufficient to break up the large drop and this drop grows even larger with accumulating secondary droplets. The behavior of the secondary spray described above is summarized in the following table.

Table 1. Mode Changes: n = no secondary spray, j = film jetting, d = droplet formation, s = common secondary spray

flow rate	-20g	-16g	-12g	-8g	-4g	-2g	0g	2g	4g	8g	12g	16g	20g
0.65	j	s	s	s	s	s	s	s	s	s	s		
0.55	j	j	s	s	s	d	s	s	s	s	s	s	s
0.45	j	j	j	j	d	d	s	s	s	s	s	s	s
0.35	j	j	j	j	j	j	s	s	s	s	s	s	s
0.25	n	j	j	j	j	j	s	s	s	s	s	s	s

Conclusions

The dynamics of the liquid film produced by spray impact under various gravity levels have been investigated by using high-speed visualization and image processing and compared to previous results obtained under microgravity and terrestrial conditions. Different breakup mechanisms and mode changes of the secondary spray have been identified. In addition, typical parameters of the impacting spray, such as the average drop velocity, have been estimated.

Nomenclature

g gravity
U_a *average drop velocity*
m *mass*
$\acute{v}g$ hypergravity
ω angular rotation rate if centrifuge

Subscripts
g gas

l liquid

Superscripts
+ positive g-level
- negative g-level

References

1. Mudawar, I., and Deiters, T.A., *Int. J. Heat Mass Transfer* 37: 347-362 (1994)
2. Hall, D.D., and Mudawar, I., *Int. J. Heat Mass Transfer* 38: 1201-1216 (1995)
3. Celata, G.P., Colin, C., Colinet, P., Dimarco, P., Gambaryan-Roisman, T., Kabov, O., Kyriopoulos, O., Stephan, P., Tadrist, L., and Tropea, C., *Europhysics News* 39, 4: 23-25 (2008)
4. Roisman, I.V., Horvat, K., and Tropea, C., *Phys. Fluids* 18: 102 (2006)
5. Roisman, I.V., Gambaryan-Roisman, T., Kyriopoulos, O., Stephan, P., Tropea, C., *Phys. Rev. E* 76: 026302 (2007)
6. Cossali, G.E., Marengo, M., and Santini, M., *Atomization and Sprays* 15: 699 (2005)
7. Tropea, C., and Roisman, I.V., *Atomization and Sprays* 10: 387 (2000)
8. Kyriopoulos, O., Roisman, I.V., Gambaryan-Roisman, T., Stephan, P., and Tropea, C., *Jap. Soc. Micro. Appl. Journal* 25, 3: 231-234 (2008)
9. Kyriopoulos, O., Roisman, I.V., Gambaryan-Roisman, T., Stephan, P. and Tropea, C., *22nd European Conference on Liquid Atomization and Spray Systems,* Como Lake, Italy, September 8-10, pp. 13-15.
10. Gambaryan-Roisman, T., Kyriopoulos, O., Roisman, I.V., Stephan, P., Tropea, C., *Micro. Sci. Technol. Int. Journal* 19, 3-4: 151-154 (2007)